

Regular black hole in three dimensions

Yun Soo Myung*

*Institute of Basic Science and School of Computer Aided Science,
Inje University, Gimhae 621-749, Korea*

Myungseok Yoon†

Center for Quantum Spacetime, Sogang University, Seoul 121-742, Korea

(Dated: November 4, 2018)

Abstract

We find a new black hole in three dimensional anti-de Sitter space by introducing an anisotropic perfect fluid inspired by the noncommutative black hole. This is a regular black hole with two horizons. We compare thermodynamics of this black hole with that of non-rotating BTZ black hole. The first-law of thermodynamics is not compatible with the Bekenstein-Hawking entropy.

PACS numbers: 04.70.Dy,97.60.Lf

Keywords: Regular black hole, black hole thermodynamics

arXiv:0810.0078v2 [gr-qc] 9 Apr 2009

*Electronic address: ysmyoung@inje.ac.kr

†Electronic address: younms@sogang.ac.kr

I. INTRODUCTION

Hawking's semiclassical analysis of the black hole radiation suggests that most information about initial states is shielded behind the event horizon and will not back to the asymptotic region far from the evaporating black hole [1]. This means that the unitarity is violated by an evaporating black hole. However, this conclusion has been debated by many authors for three decades [2, 3, 4]. It is closely related to a long standing puzzle of the information loss paradox, which states the question of whether the formation and subsequent evaporation of a black hole is unitary. One of the most urgent problems in black hole physics is to resolve the unitarity issue. In this direction, a complete description of black hole evaporation is an important issue. In order to determine the final state of evaporation process, a more precise treatment including quantum gravity effects and backreaction is generally required. At present, two leading candidates for quantum gravity are the string theory and the loop quantum gravity. Interestingly, the semiclassical analysis of the loop quantum black hole provides a regular black hole (RBH) without singularity whose minimum size r_c is at Planck scale l_p , in contrast to the classical one [5].

RBHs have been considered, dating back to Bardeen [6], for avoiding the curvature singularity beyond the event horizon in black hole physics [7]. Their causal structures are similar to the Reissner-Nordström black hole with the singularity replaced by de Sitter space-time with curvature radius $\tilde{r}_0 = \sqrt{3/\Lambda}$ [8, 9]. Hayward has discussed the formation and evaporation process of a RBH with minimum size l [10] which can be identified with the minimal length induced from the string theory [11], and its thermodynamic analysis was performed in [13]. A rigorous treatment of the evaporation process was carried out for the renormalization group (RG) improved black hole with minimum size $r_{cr} = \sqrt{\tilde{\omega}G}$ [12].

On the other hand, the noncommutativity with parameter θ may provide another RBH with minimum scale $\sqrt{\theta}$: noncommutative black hole [14, 15, 16] and its commutative limit is the Schwarzschild black hole. Recently, the authors [17] have investigated thermodynamics and evaporation process of this noncommutative black hole. The thermodynamics similarity between the noncommutative and Reissner-Nordström black holes was shown in Ref.[18]. The entropy issue of this black hole was discussed in [19, 20] and the Hawking radiation was considered in [21]. The connection between their minimum sizes is given by $r_c \sim \tilde{r}_0 \sim l \sim r_{cr} \sim \sqrt{\theta} \sim l_p$.

In this work, we construct a new black hole in AdS₃ spacetimes by introducing an anisotropic perfect fluid inspired by the 4D noncommutative black hole. This is a regular black hole with two horizons in three dimensions. We compare thermodynamics of this black hole with that of non-rotating BTZ black hole (NBTZ). The first-law of thermodynamics is not compatible with the Bekenstein-Hawking entropy. Finally, we discuss thermodynamics of 3D noncommutative black holes based on the Gaussian distribution.

II. 3D REGULAR BLACK HOLE

We start with a cylindrically symmetric line element in three dimensions

$$ds^2 = -f(r)dt^2 + f(r)^{-1}dr^2 + r^2d\phi^2, \quad (1)$$

where f is the metric function to be determined.

It has been shown [14] that the noncommutativity eliminates point-like structures in favor of smeared objects in flat spacetime. A way of implementing the effect of smearing is a substitution rule: in four-dimensional (4D) spacetimes, Dirac-delta function $\delta_{4D}(r)$ is replaced by a Gaussian distribution of the minimal width $\sqrt{\theta}$ [14, 15, 17] as

$$\rho_{\theta}^{4D}(r) = \frac{M}{(4\pi\theta)^{3/2}} e^{-r^2/4\theta} \quad (2)$$

whose mass distribution is defined by

$$m_{\theta}^{4D}(r) = \int_0^r 4\pi r'^2 \rho_{\theta}^{4D}(r) dr' = \frac{2M}{\sqrt{\pi}} \gamma(3/2, r^2/4\theta). \quad (3)$$

Here $\gamma(3/2, r^2/4\theta)$ is the lower incomplete gamma function defined as defined by

$$\gamma(a, z) = \int_0^z t^{a-1} e^{-t} dt. \quad (4)$$

In the limit of $r^2/4\theta \rightarrow \infty$, one finds $m_{\theta}^{4D} \rightarrow M$.

In three dimensions, Dirac-delta function $\delta_{3D}(r)$ is replaced by a Gaussian distribution of the minimal width $\sqrt{\theta}$ as

$$\rho_{\theta}^{3D}(r) = \frac{M}{4\pi\theta} e^{-r^2/4\theta} \quad (5)$$

whose mass distribution is simply calculated to be

$$m_{\theta}^{3D}(r) = \int_0^r 2\pi r' \rho_{\theta}^{3D}(r) dr' = M\gamma(1, r^2/4\theta) = M(1 - e^{-r^2/4\theta}). \quad (6)$$

In the limit of $r^2/4\theta \rightarrow \infty$, one recovers $m_\theta^{3D} \rightarrow M$ easily.

The Gaussian distribution (5) may be suitable for describing a three-dimensional (3D) noncommutative black hole. However, we will show in Sec. VI that this choice makes an difficulty to define a small black hole. It turns out that the 3D noncommutative black hole does not have two horizons and it takes a degenerate horizon at the origin $r = 0$. However, the small 3D noncommutative black hole is not defined in the limit of $r_H \rightarrow 0$ because a smeared (Gaussian) distribution around the origin is not appropriate to make a small black hole.

On the other hand, the 4D noncommutative black hole has two horizons and thus it becomes an extremal black hole for $r_C = r_E$. As far as concerned on the study of thermodynamics of black holes, the relevant region to observer at infinity is outside the degenerate horizon. Hence it is promising to obtain a 3D black hole with two horizons. For this purpose, we wish to look for a different mass distribution which may offer m_θ^{4D} in Eq.(3).

To this end, we compare the 4D Poisson equation of $\partial_r^2(1/r) \sim \delta_{4D}(r)$ with 3D equation $\partial_r^2(\ln r) \sim \delta_{3D}(r)$. Considering the relation of $\partial_r \ln r = 1/r$, a quantity of $\partial_r e^{-r^2/4\theta} \sim 2re^{-r^2/4\theta}$ is a similar object in 3D spacetimes. Hence, we introduce a new mass density of cylindrically symmetric, smeared gravitational source as

$$\rho_\theta(r) = \frac{Mr}{4(\pi\theta)^{3/2}} \exp\left(-\frac{r^2}{4\theta}\right) \quad (7)$$

whose mass distribution mimics the 4D mass distribution m_θ^{4D} as

$$m_\theta(r) = \int_0^r 2\pi r' \rho_\theta(r) dr' = \frac{2M}{\sqrt{\pi}} \gamma(3/2, r^2/4\theta). \quad (8)$$

We note that this mass distribution differs from the m_θ^{3D} in Eq.(6) for the 3D noncommutative black hole. This choice is meaningful for a 3D smeared gravitational source because it provides a regular black hole with two horizons. For another 3D noncommutative BTZ black hole, see Ref.[22].

In order to find a black hole solution in AdS₃ spacetime, we introduce the Einstein equation

$$R_{\mu\nu} - \frac{1}{2}Rg_{\mu\nu} = 8\pi T_{\mu\nu} + \Lambda g_{\mu\nu}, \quad \text{with } \Lambda = 1/\ell^2, \quad (9)$$

where the energy-momentum tensor takes an anisotropic form

$$T^\mu{}_\nu = \text{diag}(-\rho_\theta, p_r, p_\perp). \quad (10)$$

The Bianchi identity is satisfied ($T^\mu{}_\nu$ is conserved) if the radial pressure p_r and tangential pressure p_\perp satisfy the relations, respectively

$$p_r = -\rho_\theta, \quad p_\perp = -\rho_\theta - r\rho_\theta', \quad (11)$$

where $'$ denotes the derivative with respect to r . Components of Einstein equation are given by

$$(tt) \text{ or } (rr) : \frac{f'}{2r} = -8\pi\rho_\theta + \frac{1}{\ell^2} \quad (12)$$

$$(\phi\phi) : \frac{1}{2}f'' = 8\pi p_\perp + \frac{1}{\ell^2}. \quad (13)$$

Solving the above equations determines the metric function to be

$$f(r, \theta) = \frac{r^2}{\ell^2} - \frac{16M}{\sqrt{\pi}}\gamma\left(\frac{3}{2}, \frac{r^2}{4\theta}\right) = \frac{r^2}{\ell^2} - 8m_\theta(r). \quad (14)$$

We note that $r^2/4\theta \rightarrow \infty$, when either $r \rightarrow \infty$ or $\theta \rightarrow 0$. The former corresponds to the large black hole, while the latter corresponds to the commutative limit. In the limit of $r^2/4\theta \rightarrow \infty$, one finds $\gamma(3/2, \infty) = \sqrt{\pi}/2$ which leads to the metric function for the NBTZ

$$f_{NBTZ}(r) = \frac{r^2}{\ell^2} - 8M. \quad (15)$$

In order to obtain a black hole solution, we find the solution to $f = 0$ numerically. Two horizons come together at the value of mass $M = M_*$, which puts a lower limit on the black hole mass. For given θ , the horizon of extremal black hole is determined from the conditions of $f = 0$ and $f' = 0$ as

$$\frac{r_*}{2\sqrt{\theta}} = \alpha, \quad (16)$$

where $\alpha = 0.9679$ is the value satisfying

$$\gamma\left(\frac{3}{2}, \alpha^2\right) = \alpha^3 e^{-\alpha^2}. \quad (17)$$

This implies that the minimal length of regular black hole is $r_* \simeq 2\sqrt{\theta}$. As is shown in Fig. 1, for $M < M_*$ there is no solution to $f = 0$ while for $M > M_*$ there exist two horizons: the cosmological horizon r_C and event horizon r_H . The corresponding density profiles are depicted in Fig. 2. Then, the mass of the extremal black hole is determined from the condition of $f(r_*, \theta) = 0$ to be

$$M_*(\theta) = \frac{\sqrt{\pi}e^{\alpha^2}}{4\alpha\ell^2}\theta. \quad (18)$$

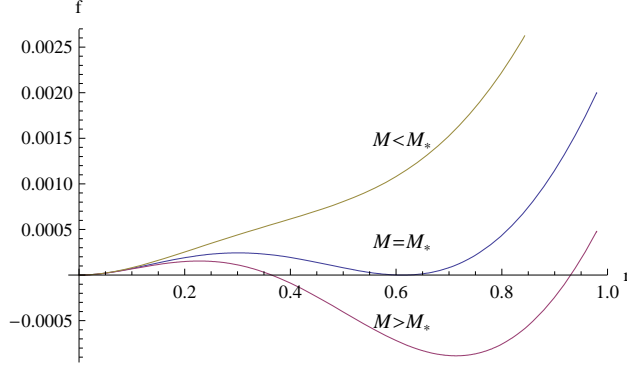


FIG. 1: Metric function f as function of r with $\theta = 0.1$ and $\ell = 10$. For $M = M_* = 0.0012$, the degenerate horizon is located at $r_* = 0.6121$, while for $M > M_*$, the black hole appears with the inner horizon $r_C = 0.3647$ and the outer horizon $r_H = 0.9304$. For $M < M_*$, there is no black hole.

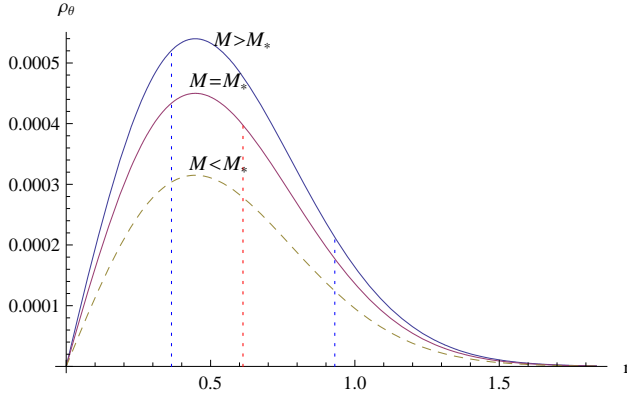


FIG. 2: The density profiles $\rho_\theta(r)$ are plotted for different mass M . When $M < M_*$, the black hole cannot be formed (dashed line). There is an extremal black hole with horizon at $r = r_*$ for $M = M_*$ and a black hole with the inner horizon ($r_C = 0.3647$) and outer horizon ($r_H = 0.9304$) for the mass $M = 0.0014$.

The whole picture is given by Fig. 3. At $\theta = 0$, we find a massless BTZ black hole with $M = 0$ and the NBTZ with $M \neq 0$. In case of $\theta \neq 0$ (dashed vertical line), we have regular black hole for $M > M_*$, extremal black hole at $M = M_*$ and AdS₃ spacetime for $M < M_*$.

From the condition of $f = 0$, the mass function of horizon radii r_C and r_H is given by

$$M(r_{C/H}, \theta) = \frac{\sqrt{\pi}}{16\ell^2} \frac{r_{C/H}^2}{\gamma\left(\frac{3}{2}, \frac{r_{C/H}^2}{4\theta}\right)}. \quad (19)$$

In the limit of $\theta \rightarrow 0$, one finds the mass function for NBTZ as

$$M(r_H, \theta \rightarrow 0) = \frac{r_H^2}{8\ell^2}. \quad (20)$$

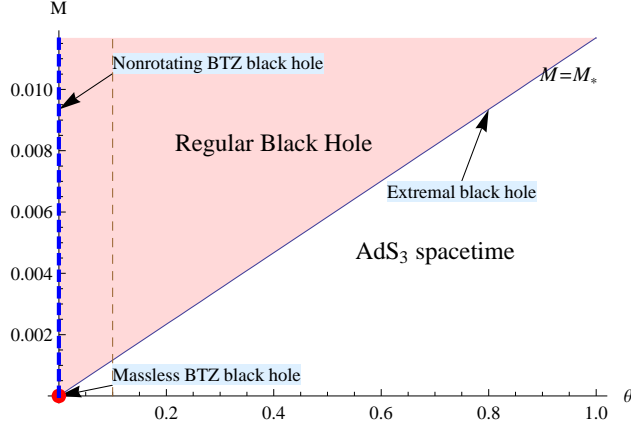


FIG. 3: Mass M versus θ with $\ell = 10$. The extremal black hole is described by $M = M_*(\theta)$. For given θ , the regular black holes appear for $M > M_*$, while for $M < M_*$, the spacetimes is just the pure AdS_3 space. The M -axis ($\theta = 0$) represents the NBTZ.

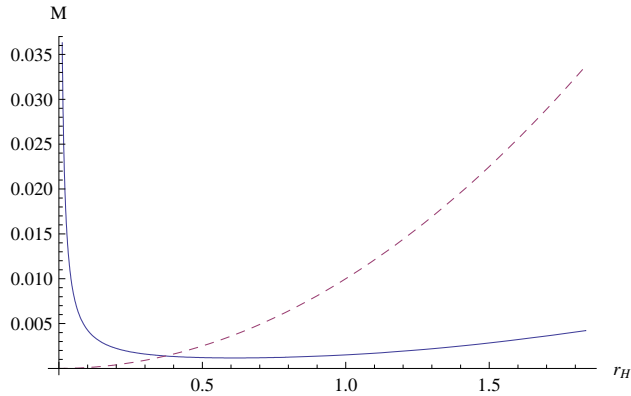


FIG. 4: Mass versus r_C and r_H . Solid curve: for $r \leq r_* = 0.6121$, one uses $r = r_C$, while for $r \geq r_*$, one uses $r = r_H$. The minimum mass $M = M_*$ occurs at $r_C = r_H = r_*$. Dashed curve represents the mass as function of r_H for the NBTZ.

These are depicted in Fig. 4.

Three conditions for the existence of regular black hole in AdS_3 spacetimes are checked [8]:
i) regularity of the metric function $f(r)$ and energy density $\rho_\theta(r)$ at the origin of coordinate $r = 0$. ii) asymptotically AdS spacetimes and the finiteness of ADM mass ($M < \infty$). iii) dominated energy condition for the energy-momentum tensor $T_{\mu\nu}$ in Eq. (10). However, from Fig. 2, one finds that $\rho_\theta' > 0$ for $r < r_m$ and $\rho_\theta' < 0$ for $r > r_m$, where $r_m = \sqrt{2\theta} < r_*$ is the maximum value determined by $\rho_\theta' = 0$. The dominant energy condition of $T^{00} \geq |T^{ab}|$ ($a, b = 1, 2$) is equivalent to $\rho_\theta \geq 0 \wedge -\rho_\theta \leq p_r \leq \rho_\theta \wedge -\rho_\theta \leq p_\perp \leq \rho_\theta$ [9].

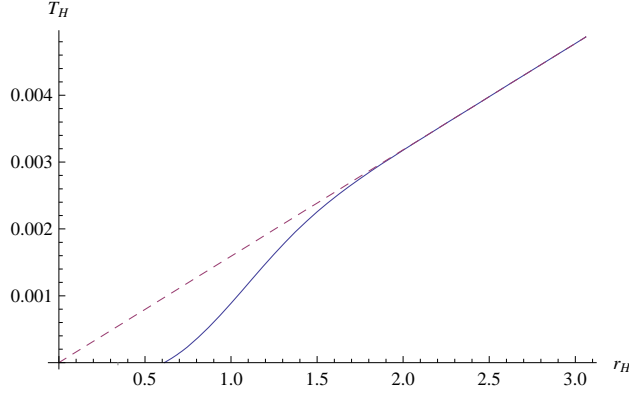


FIG. 5: Hawking temperature versus r_H with $\ell = 10$. The solid curve represents $T_H(r_H, \theta = 0.1)$, while the dashed line denotes $T_H(r_H, \theta \rightarrow 0)$ for the NBTZ.

Hence, $T_{\mu\nu}$ violates the dominant energy condition for $r < r_m$. The weak energy condition of $T_{\mu\nu}\xi^\mu\xi^\nu \geq 0$ for any timelike vector ξ^μ is equivalent to $\rho_\theta \geq 0 \wedge \rho_\theta + p_r \geq 0 \wedge \rho_\theta + p_\perp \geq 0$. Also, $T_{\mu\nu}$ violates the weak energy condition for $r < r_m$. Finally, the strong energy condition of $\rho_\theta + p_r + p_\perp \geq 0 \wedge \rho_\theta + p_r \geq 0 \wedge \rho_\theta + p_\perp \geq 0$ is violated for $r < r_m$.

III. THERMODYNAMICS OF 3D REGULAR BLACK HOLE

From the condition of $T_H = f'(r_H, \theta)/4\pi$, we obtain the Hawking temperature

$$T_H(r_H, \theta) = \frac{r_H}{2\pi\ell^2} \left[1 - \left(\frac{r_H^2}{4\theta} \right)^{\frac{3}{2}} \frac{\exp\left(-\frac{r_H^2}{4\theta}\right)}{\gamma\left(\frac{3}{2}, \frac{r_H^2}{4\theta}\right)} \right]. \quad (21)$$

For $\theta = 0.1$, we have the temperature, showing the deviation from $T_H(r_H, \theta \rightarrow 0) = r_H/2\pi\ell^2$ of the NBTZ for small r_H . The temperature is a monotonically increasing function of horizon radius for large r_H . Also, we observe that $T_H(r_*, \theta) = 0$ at $r_H = r_*$, indicating the zero temperature for the extremal black hole.

There are two ways to define the entropy. First we introduce the Bekenstein-Hawking entropy with $G_3 = 1$

$$S_{BH} = \frac{\pi r_H}{2}. \quad (22)$$

Unfortunately, this choice does not satisfy the first-law of thermodynamics

$$dM \neq T_H dS_{BH}, \quad (23)$$

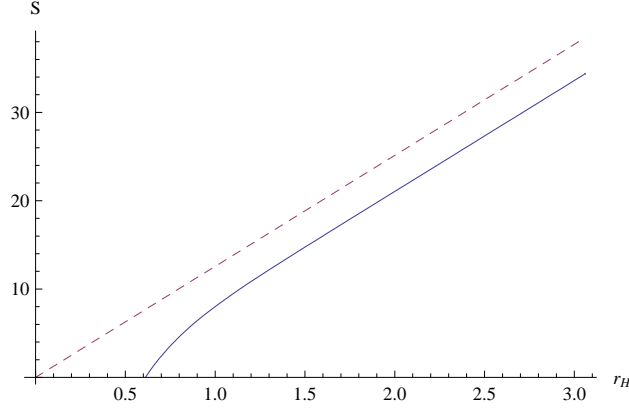


FIG. 6: Entropy versus horizon radius r_H . The solid curve and dashed line show the entropy $S(r_H, \theta = 0.1)$ of regular black hole and $S(r_H, \theta \rightarrow 0) = S_{BH}$ of NBTZ, respectively.

while it satisfies the area-law. On the other hand, we require that the first-law be satisfied with the regular black hole. Then, we obtain the entropy by integrating $dM = T_H dS$ over r_H as

$$S(r_H, \theta) = \int_{r_*}^{r_H} \frac{1}{T_H} \left(\frac{dM}{dr'_H} \right) dr'_H = \frac{\pi^{3/2}}{4} \int_{r_*}^{r_H} \frac{dr'_H}{\gamma\left(\frac{3}{2}, \frac{r'^2_H}{4\theta}\right)}. \quad (24)$$

However, this entropy does not satisfy the area-law. The behavior of the entropy is depicted in Fig. 6. In the limit of $\theta \rightarrow \infty$, one finds that $S(r_H, \theta \rightarrow 0) = (\pi/2) \int_0^{r_H} dr'_H = S_{BH}$.

The heat capacity is defined as

$$C(r_H, \theta) = \left(\frac{\partial M}{\partial T_H} \right)_\theta = \left(\frac{\partial M}{\partial r_H} \right)_\theta \left(\frac{\partial T_H}{\partial r_H} \right)_\theta^{-1}. \quad (25)$$

The heat capacity determines the thermodynamic stability. For $C > 0$, the black hole is locally stable, while for $C < 0$, the corresponding black hole is locally unstable. As is shown Fig. 7, the regular black hole has a single stable phase, similar to $C(r_H, \theta \rightarrow 0) = \pi r_H/2$ of NBTZ. For large r_H , two black holes have the nearly same heat capacity.

Finally we define the on-shell free energy

$$F(r_H, \theta) = M(r_H, \theta) - M_*(\theta) - T_H(r_H, \theta)S(r_H, \theta). \quad (26)$$

Here we use the extremal black hole as the ground state [23], even though there is no gauge field. This is mainly because the extremal black hole plays the role of a stable remnant in the regular black hole. The free energy is shown in Fig. 8. In the limit of $\theta \rightarrow 0$, one has the free energy $F(r_H, \theta \rightarrow 0) = -r_H^2/8\ell^2$ of NBTZ. Also we observe that $F(r_*, \theta) = 0$, showing the

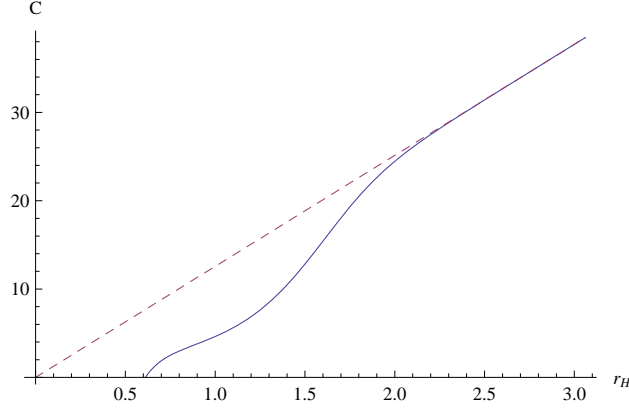


FIG. 7: The solid curve and dashed line show the heat capacity $C(r_H, \theta = 0.1)$ of regular black hole and $C(r_H, \theta \rightarrow 0)$ of NBTZ, respectively.

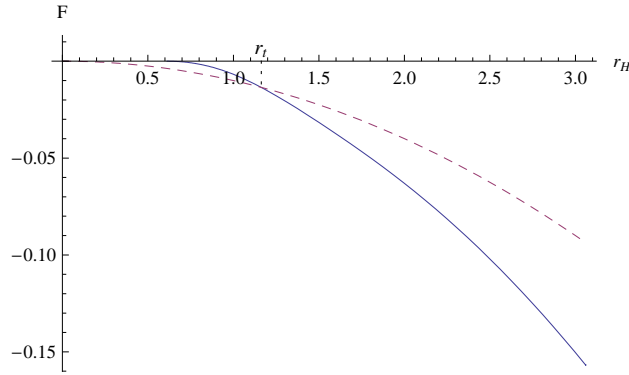


FIG. 8: Free Energy versus the horizon radius r_H . The solid and dashed curves show the free energy $F(r_H, \theta = 0.1)$ of regular black hole and $F(r_H, \theta \rightarrow 0)$ of NBTZ, respectively.

zero free energy for the extremal black hole. Importantly, there is a nonvanishing probability for decay of regular black hole into NBTZ for $r_H < r_t$ where r_t is determined by the condition of $F(r_t, \theta) = F(r_t, \theta \rightarrow 0)$, because of $F(r_t, \theta) > F(r_t, \theta \rightarrow 0)$ [24, 25]. On the other hand, for $r_H > r_t$, there is a nonvanishing probability for decay of NBTZ to regular black hole because of $F(r_t, \theta) < F(r_t, \theta \rightarrow 0)$.

IV. 3D NONCOMMUTATIVE BLACK HOLE

Considering the 3D Gaussian distribution (5), the metric function is obtained as

$$f_{\theta}^{3D}(r) = \frac{r^2}{\ell^2} - 8m_{\theta}^{3D}(r) = \frac{r^2}{\ell^2} - 8M \left(1 - e^{-\frac{r^2}{4\theta}} \right). \quad (27)$$

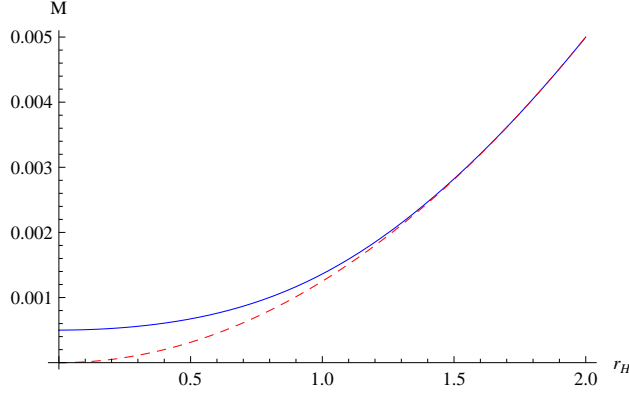


FIG. 9: The mass M as a function of horizon radius r_H . The solid and the dashed line indicate the 3D noncommutative black hole and NBTZ, respectively. These black holes have single horizon except $r_H = 0$.

From the condition of $f_\theta^{3D}(r_H) = 0$, the mass takes the form

$$M = \frac{r_H^2}{8\ell^2 \left[1 - \exp\left(-\frac{r_H^2}{4\theta}\right) \right]}. \quad (28)$$

We note that this black hole has single horizon except $r_H = 0$. Observing the metric function (27) leads to that $f_\theta^{3D} \rightarrow 0$, as $r \rightarrow 0$, irrespective of whatever M is taken. This implies that the mass is not correctly defined in the limit of $r_H \rightarrow 0$. Using the L'Hospital principle, it may lead to $M \rightarrow \frac{\theta}{2\ell^2}$ in the limit of $r_H \rightarrow 0$. Thus, we may obtain Fig. 9. However, this value does not reflect the correct limit because we could not define the 3D noncommutative black hole in the limit of $r_H \rightarrow 0$. This uncertainty propagates all thermodynamic quantities.

The Hawking temperature is computed to be

$$T_H = \frac{r_H}{2\pi\ell^2} \left[1 + \frac{r_H^2}{4\theta \left(1 - \exp\left(\frac{r_H^2}{4\theta}\right) \right)} \right]. \quad (29)$$

We note that the temperature takes an indeterminate form of $\frac{0}{0}$ at $r_H = 0$, even though it appears determinate in Fig. 10.

The entropy is obtained as

$$S = \int_{r_0}^{r_H} \frac{dM}{T_H} = \frac{\pi}{2} \int_{r_0}^{r_H} \frac{d\xi}{1 - \exp\left(-\frac{\xi^2}{4\theta}\right)}, \quad (30)$$

where $r_0 = 0.4$ is chosen for given $\theta = 0.1$ and $\ell = 10$ by requiring the condition of the consistency with the entropy $S_{BH} = \pi r_H/2$ of NBTZ for a large black hole (Fig. 11). For a small black hole, the entropy is not properly defined as $S \approx 2\pi\theta(1/r_0 - 1/r_H)$.

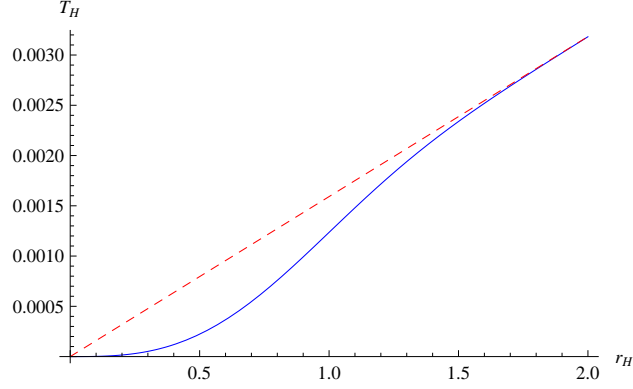


FIG. 10: This figure shows the profile of the Hawking temperature. The solid and the dashed line indicate the 3D noncommutative black hole and NBTZ, respectively.

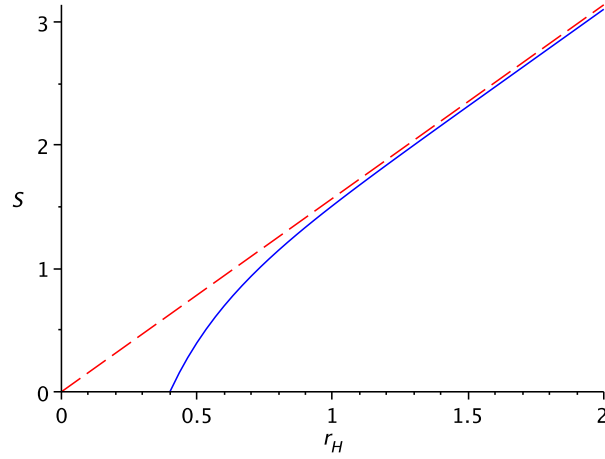


FIG. 11: This figure denotes the behavior of the entropy. The solid and the dashed line indicate the 3D noncommutative black hole and NBTZ, respectively.

The heat capacity is calculated as

$$C = \frac{\partial M}{\partial T_H} = \frac{\partial M}{\partial r_H} \left(\frac{\partial T_H}{\partial r_H} \right)^{-1} \quad (31)$$

$$= \frac{\pi r_H}{2} \frac{1 - \left(1 + \frac{r_H^2}{4\theta}\right) e^{-\frac{r_H^2}{4\theta}}}{1 + e^{-\frac{r_H^2}{4\theta}} \left[-2 \left(4 - \frac{r_H^2}{4\theta}\right) \left(1 + \frac{r_H^2}{4\theta}\right) + \left(1 + \frac{3r_H^2}{4\theta}\right) e^{-\frac{r_H^2}{4\theta}} \right]}, \quad (32)$$

which shows an unusual behavior $C \sim 2\pi\theta/(3r_H)$ for small r_H (See Fig. 12), comparing with $C_{NBTZ} = \pi r_H/2$.

The free energy is given by

$$F = M(r_H) - T_H S(r_H), \quad (33)$$

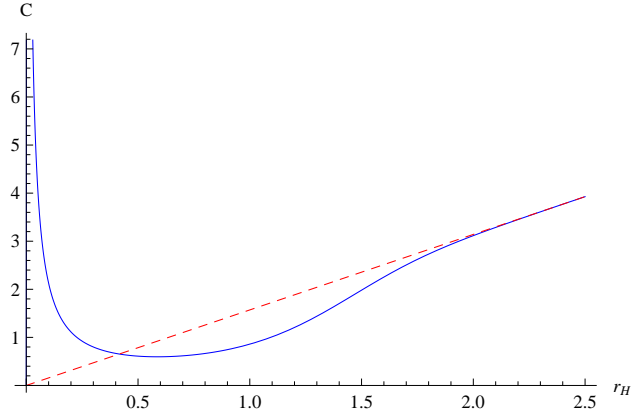


FIG. 12: This shows the heat capacity, which is positive definite. The solid and the dashed line indicate the 3D noncommutative black hole and NBTZ, respectively.

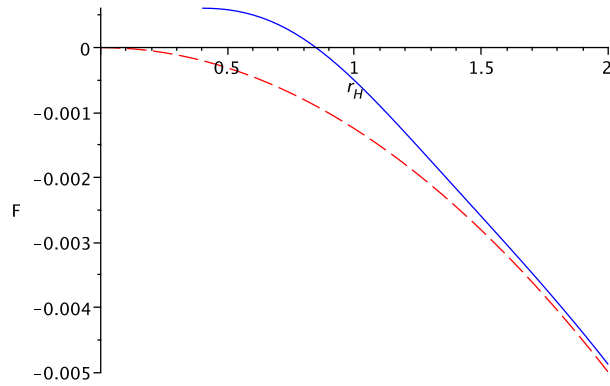


FIG. 13: This indicates the free energy. The solid and the dashed line indicate the 3D noncommutative black hole and NBTZ, respectively.

As is shown in Fig. 13, we could not define the free energy for small black holes, because there exist uncertainties for M , T_H , and S_{BH} for small black holes.

V. DISCUSSION

We construct a regular black hole in AdS_3 spacetimes by introducing an anisotropic perfect fluid (10) inspired by the 4D noncommutative black hole. This black hole has a nature of the 4D noncommutative black hole with two horizons in three dimensions.

We compare thermodynamics of this black hole with that of non-rotating BTZ black hole (NBTZ). The Hawking temperature and heat capacity of large regular black hole approach

those of NBTZ. However, the entropy of regular black hole is different from the Bekenstein-Hawking entropy of NBTZ because we use the first-law of thermodynamics to derive the entropy. Actually, it confirms that the first-law of thermodynamics is not compatible with the Bekenstein-Hawking entropy for regular black holes.

From the graph of free energy in Fig. 8, we observe that there is a nonvanishing probability for decay of regular black hole into NBTZ for $r_H < r_t$, while for $r_H > r_t$, there is a nonvanishing probability for decay of NBTZ to regular black hole. This implies that there may exist a phase transition between regular black hole and NBTZ.

On the other hand, the Gaussian distribution (5) provides the 3D noncommutative black hole with single horizon except $r_H = 0$. The thermodynamics of small 3D noncommutative black hole is not well established. The small 3D noncommutative black hole is not defined in the limit of $r_H \rightarrow 0$ since the a smeared (Gaussian) distribution around the origin is not appropriate to make a small black hole, differing from the point Dirac-delta function.

Acknowledgments

This work was supported by the Science Research Center Program of the Korea Science and Engineering Foundation through the Center for Quantum Spacetime (CQUeST) of Sogang University with grant number R11-2005-021.

-
- [1] S. W. Hawking, Phys. Rev. D **14**, 2460 (1976).
 - [2] G. 't Hooft, Nucl. Phys. B **335**, 138 (1990).
 - [3] L. Susskind, hep-th/0204027.
 - [4] D. N. Page, New J. Phys. **7**, 203 (2005).
 - [5] L. Modesto, hep-th/0701239.
 - [6] J. Bardeen, in Proceedings of GR5, Tbilisi, U.S.S.R, 1968, p174.
 - [7] A. Borde, Phys. Rev. D **50**, 3692 (1994);
E. Ayon-Beato and A. Garcia, Phys. Rev. Lett. **80**, 5056 (1998).
 - [8] I. Dymnikova, Gen. Rel. Grav. **24**, 235 (1992);
I. Dymnikova, Int. J. Mod. Phys. D **12**, 1015 (2003).

- [9] S. Ansoldi, arXiv:0802.0330 [gr-qc].
- [10] S. A. Hayward, Phys. Rev. Lett. **96**, 031103 (2006).
- [11] G. Veneziano, Europhys. Lett. **2**, 199 (1986);
D. J. Gross and P. F. Mende, Nucl. Phys. B **303**, 407 (1988).
- [12] A. Bonanno and M. Reuter, Phys. Rev. D **73**, 083005 (2006).
- [13] Y. S. Myung, Y. W. Kim and Y. J. Park, Phys. Lett. B **656**, 221 (2007).
- [14] A. Smailagic and E. Spallucci, J. Phys. A **36**, L467 (2003);
T. G. Rizzo, J. High Energy Phys. **09**, 021 (2006).
- [15] P. Nicolini, A. Smailagic, and E. Spallucci, Phys. Lett. B **632**, 547 (2006);
S. Ansoldi, P. Nicolini, A. Smailagic and E. Spallucci, Phys. Lett. B **645**, 261 (2007);
E. Spallucci, A. Smailagic and P. Nicolini, Phys. Lett. B **670** (2009) 449 [arXiv:0801.3519
[hep-th]].
- [16] P. Nicolini, arXiv:0807.1939 [hep-th].
- [17] Y. S. Myung, Y. W. Kim and Y. J. Park, JHEP **0702**, 012 (2007).
- [18] W. Kim, E. J. Son and M. Yoon, JHEP **0804**, 042 (2008).
- [19] R. Banerjee, B. R. Majhi and S. Samanta, Phys. Rev. D **77**, 124035 (2008).
- [20] R. Banerjee, B. R. Majhi and S. K. Modak, arXiv:0802.2176 [hep-th].
- [21] K. Nozari and S. H. Mehdipour, Class. Quant. Grav. **25**, 175015 (2008).
- [22] H. C. Kim, M. I. Park, C. Rim and J. H. Yee, JHEP **0810** (2008) 060 [arXiv:0710.1362
[hep-th]].
- [23] A. Chamblin, R. Emparan, C. V. Johnson and R. C. Myers, Phys. Rev. D **60**, 064018 (1999).
- [24] C. Martinez, R. Troncoso and J. Zanelli, Phys. Rev. D **70**, 084035 (2004).
- [25] Y. S. Myung, Phys. Lett. B **663**, 111 (2008).